Organic Matter Controls of Iron Incorporation in Growing Sea Ice

Julie Janssens [1,2,3*], Klaus M. Meiners [2,3], Ashley T. Townsend [4] and Delphine Lannuzel [1,2]

[1] Institute for Marine and Antarctic Studies, University of Tasmania, Hobart, TAS, Australia, [2] Antarctic Climate and Ecosystems Cooperative Research Centre, University of Tasmania, Hobart, TAS, Australia, [3] Australian Antarctic Division, Department of the Environment and Energy, Kingston, TAS, Australia, [4] Central Science Laboratory, University of Tasmania, Hobart, TAS, Australia

This study presents the first laboratory-controlled sea-ice growth experiment conducted under trace metal clean conditions. The role played by organic matter in the incorporation of iron (Fe) into sea ice was investigated by means of laboratory ice-growth experiments using a titanium cold-finger apparatus. Experiments were also conducted to understand the role of extracellular polymeric substances (EPS) in the enrichment of ammonium in sea ice. Sea ice was grown from several seawater solutions containing different quantities and qualities of particulate Fe (PFe), dissolved Fe (DFe) and organic matter. Sea ice and seawater were analyzed for particulate organic carbon and nitrogen, macro-nutrients, EPS, PFe, and DFe, and particulate aluminum. The experiments showed that biogenic PFe is preferentially incorporated into sea ice compared to lithogenic PFe. Furthermore, sea ice grown from ultra-violet (UV) and non-UV treated seawaters exhibits contrasting incorporation rates of organic matter and Fe. Whereas, the effects of UV-treatments were not always significant, we do find indications that the type or organic matter controls the enrichment of Fe in forming sea ice. Specifically, we come to the conclusion that the incorporation of DFe is favored by the presence of organic ligands in the source solution.

Keywords: sea ice, iron, EPS, organic matter, organic ligands, incorporation, Antarctica

INTRODUCTION

Sea ice is an important reservoir of iron (Fe) in the Southern Ocean (e.g., Sedwick and DiTullio, 1997; Lancelot et al., 2009; Lannuzel et al., 2010; Wang et al., 2014). Every spring, Fe contained in sea ice is released into surface waters and can trigger phytoplankton blooms in the marginal ice zone. This seasonal event represents an important source of food for higher trophic levels and potentially contributes to the biological pump in the Southern Ocean (Sullivan et al., 1993; Lannuzel et al., 2007, 2010). Climate predictions suggest sea-ice extent and volume will decrease by 24 and 34%, respectively by 2100 (Arzel et al., 2006). The effect of these changes on sea-ice biogeochemical processes, and most importantly on the uptake of carbon dioxide (CO_2) in the Southern Ocean, remains enigmatic. It is therefore of primary importance to gain a mechanistic understanding of the processes leading to Fe enrichment in sea ice. This step is necessary to adequately represent ice-associated iron biogeochemistry in numerical models.

The co-occurrence of enrichment of organic matter and Fe in sea ice suggests that they are coupled (Grotti et al., 2005; Lannuzel et al., 2007, 2008, 2014a; van der Merwe et al., 2009, 2011a,b; de Jong et al., 2013, 2015; Janssens et al., 2016). It has been proposed that the Fe

concentration in the ice depends on the Fe concentration in the parent seawater during sea-ice formation (van der Merwe et al., 2009). Dissolved organic ligands, potentially in the form of extracellular polymeric substances (EPS), are thought to control the distribution of dissolved Fe (DFe) in sea ice and might be a crucial vector of Fe enrichment in forming sea ice (Lannuzel et al., 2015; Genovese et al., in review).

EPS are produced by algae and bacteria (Meiners et al., 2004; Mancuso Nichols et al., 2005b; Meiners and Michel, 2017) and have been found to be enriched in sea ice compared to seawater (e.g., Krembs et al., 2002a, 2011; Meiners et al., 2003, 2004; Riedel et al., 2006; van der Merwe et al., 2009; Underwood et al., 2010; Ewert and Deming, 2011; Aslam et al., 2012; Janssens et al., 2016). EPS are a good candidate for metallic anion binding (Croot and Johansson, 2000; Verdugo et al., 2004) given their high stickiness and negatively charged surfaces (Decho, 1990; Underwood et al., 2010). EPS exist in a continuum of sizes from dissolved and colloidal to particulate fractions (Verdugo et al., 2004), and therefore may control the enrichment of all Fe size fractions in sea ice.

Janssens et al. (2016) showed that sea-ice formation leads to concomitant physical enrichment of EPS, particulate organic matter and Fe, with larger particles being preferentially enriched compared to smaller particles during an *in situ* ice-growth experiment. Nonetheless the simultaneous investigation of physical, chemical and biological processes in field conditions is extremely difficult given the complex interactions between them. In this context, laboratory ice-growth experiments are valuable to isolate specific processes. Laboratory experiments allow the formation of sea ice in a controlled environment and from chosen source solutions.

Ice tank experiments and laboratory ice-growth experiment are numerous (e.g., INTERICE experiments in Germany—e.g., Weissenberger and Grossmann, 1998; Krembs et al., 2002b; Geilfus et al., 2012; Zhou et al., 2014; CRREL experiments in the United State of America—e.g., Kovacs, 1996; Loose et al., 2009; or SERF experiments in Canada—e.g., Galley et al., 2013; Else et al., 2015). To our knowledge, none of these studies have been conducted under the trace metal clean conditions needed to study Fe-associated processes. This study aims at understanding the basic processes leading to the incorporation of Fe into growing sea ice, and specifically the role of organic matter as a carrier of Fe. Experiments were performed using a titanium (Ti) cold-finger apparatus (Kuiper et al., 2003; Ewert and Deming, 2011) tailored for use under carbon and trace metal non-contaminating conditions. Experiments were conducted to understand the role of EPS in the enrichment of ammonium (NH_4^+) in sea ice (Zhou et al., 2013) and the role of organic matter in the enrichment

of Fe in sea ice. We first hypothesize that the quality and quantity of EPS control the rate of incorporation of particulate organic carbon (POC) and NH_4^+ into sea ice. We tested this hypothesis by undertaking a set of experiments using surface water (assumed freshly formed EPS) and deep water (assumed old/preformed EPS), where we quantified the incorporation of EPS, organic matter and inorganic macro-nutrients [hereafter referred as macro-nutrients: nitrate+nitrite: $NO_2+NO_3 = NO_x$, silicic acid: $Si(OH)_4^-$, phosphate: PO_4^{3-}, and ammonium: NH_4^+)] into sea ice. Our second hypothesis was that organic matter is required to incorporate Fe into sea ice. We tested this by undertaking a second set of experiments targeting the role that organic matter plays in the enrichment of Fe (DFe and particulate Fe, PFe) into sea ice using UV and non-UV treated seawater. The addition of desert dusts and sea-ice algae in the source solutions was also carried out to investigate the difference between lithogenic and biogenic PFe incorporation in sea ice. To our knowledge, this work constitutes the first laboratory-based ice-growth experiments conducted under trace metal clean conditions.

METHODS

Experiments

Ice Texture Experiments

The first set of experiments, *Ice texture Exp.*, was conducted onboard RV *Polarstern*, and aimed at identifying the effects of different ice growth rates on ice crystal structure, i.e., ice texture. Seawater used for these experiments was collected during a winter cruise in the Weddell Sea onboard the RV *Polarstern* (ANT-XXIX/6, Lemke and Participants, 2014), using the ship water intake line. The ice was grown at −10, −15, and −20°C, for 24, 8, and 6.45 h respectively, and processed for ice texture analysis onboard the ship (**Table 1**).

Extracellular Polymeric Substances, POC, PON, and Macro-Nutrient Experiments

A second set of experiments, *EPS, POC, PON,* and *macro-nut. Exp.*, was run during the same voyage. Seawater was collected using the ship water intake line, a CTD or a peristaltic pump (E/S Portable Sampler, Masterflex) at different locations and different water depths (**Table 1**) to study the incorporation of EPS, POC, and particulate organic nitrogen (PON) and inorganic macro-nutrients ($NO_2+NO_3 = NO_x$, $Si(OH)_4^-$, PO_4^{3-}, and NH_4^+) into sea ice. The first source solution was surface seawater (Surface SW, ship water intake line). The second source solution was deep seawater (Deep SW) collected with the CTD at 4,300 m depth. In the third source solution (Surface SW + XG), 5 mg L^{-1} of xanthan gum (XG) from *Xanthomonas campestris* (Sigma-Aldrich) was added to the surface seawater sampled with a peristaltic pump (E/S Portable Sampler, Masterflex) at the ice-water interface. To achieve this, a stock solution of 1,000 mg L^{-1} XG was made and sonicated for 60 min using a Bandelin Sonopuls sonicator. The stock solution was then diluted 10 times in Ultra High Purity (UHP) water (Millipore, Gradient A10) and sonicated for 30 min before being added to the surface seawater.

Abbreviations: DFe, dissolved iron; EI, enrichment indices; EPS, extracellular polymeric substances; EPS, POC, PON and macro-nut. Exp., extracellular polymeric substances, POC, PON, and macro-nutrients experiments; Fe, iron; FEP, teflon fluorinated ethylene propylene; Ice texture Exp., ice texture experiment; Iron Exp., iron experiment; NOx, nitrate+nitrite; NH_4^+, ammonium; PAl, particulate aluminum; PFe, particulate iron; PO_4^{3-}, phosphate; POC, particulate organic carbon; PON, particulate organic nitrogen; $SiOH_4^-$, silicic acid; SW, seawater; UHP, ultra high purity; UV, ultraviolet; XG, xanthan gum; DOM, dissolved organic matter; DOC, dissolved organic carbon; CO_2, carbon dioxide.

TABLE 1 | Summary of the different cold-finger experiments.

Experiment name	Treatment name	Source solution	Addition and treatment	Freezing T (°C)	Parameters
Ice texture Exp.	Texture −10°C	RV *Polarstern* SW intake line, Weddell Sea	–	−10	Ice fabrics and dimensions of the ice formed
	Texture −15°C		–	−15	
	Texture −20°C		–	−20	
EPS, POC, PON and macro-nut. Exp.	Surface SW	RV *Polarstern* SW intake line, 67°39 S, 5°31 W	–	−15	Salinity, POC, macro-nutrients and EPS
	Deep SW	Deep SW (4,300 m), 68°01 S, 6°40 W	–		
	Surface SW + XG	Surface SW, 67°11 S, 13°14 W	5 mg/L Xanthan gum		
Iron Exp.	FSW + PFe	Pre-filtered (0.4 μm) surface SW from Trumpeter Bay, (Tasmania), 43°16 S, 147°39 E	30 μM PFe	−15	Salinity, PFe, PAl, DFe, POC, PON
	UV-FSW + PFe		30 μM PFe + 15 min UV		
	FSW + DFe		30 μM DFe		
	UV-FSW + DFe		30 μM DFe + 15 min UV		
	FSW + Algae		Sea ice algae		

In each experiment seawater was collected at different locations and different treatments were used as source solution. SW, seawater; XG, xanthan gum; POC and PON, particulate organic carbon and nitrogen; EPS, extracellular polymeric substances, FSW, filtered seawater; UV, ultra-violet; DFe, dissolved Fe; PFe, particulate Fe; PAl, particulate aluminum.

Iron Experiments

A third set of experiments, *Iron Exp.*, aimed at assessing the role of organic matter in the incorporation of Fe into growing sea ice. Experiments were conducted under trace metal clean conditions at the University of Tasmania. Surface seawater was collected on the 9th of October 2015 from Trumpeter Bay, (Tasmania: 43°16 S, 147°39 E) using a shoreline, and stored in acid-clean low-density polyethylene (LDPE, Nalgene) carboys. The sampling depth was approximately 2.5 m. In the home laboratory, seawater was filtered through polycarbonate (PC) membranes (Sterlitech, pore size: 0.4 μm) at low vacuum (<0.13 bar) using an acid-clean PC filtration apparatus (Sartorius) under a class-100 laminar flow hood (AirClean 600 PCR workstation, Model 300 Controller, AirClean System).

Filtered seawater (FSW) was divided into separate bottles for separate sets of treatments. Triplicate bottles were then spiked with different types of Fe. Added concentrations were selected to reach detectable Fe signals during analyses, despite the small volume of sea ice formed and remaining seawater. The first source solution, "FSW + PFe," was obtained by adding 30 μM of lithogenic PFe (PFe > 0.4 μm) to the FSW. Dust particles < 20 μm were used, collected in the Atacama desert, Chile (European Southern Observatory, Paranal), assuming a composition of 5% (w:w) of Fe, similar to the Earth's Crust (Taylor, 1964).

A second source solution, "FSW + DFe," was obtained by adding 30 μM of DFe (DFe < 0.4 μm) into the FSW using a commercial solution of 1,000 ppm of $FeCl_3$ (Merck).

Two complementary sets of experiments were run after UV-treatment of the FSW. This UV exposure step ensured the destruction of any dissolved organic matter (DOM) present in the solution (Queroue et al., 2014). Filtered seawater was dispensed into acid-clean 0.5 L Teflon fluorinated ethylene propylene (FEP) bottles (Nalgene) and placed between ultraviolet lamps inside a black PVC chamber for 15 min. After UV exposure, PFe or DFe

was added to the source solution following the steps adopted in treatments "FSW + PFe" and "FSW + DFe." The latter treatments are referred to as "UV-FSW + PFe" and "UV-FSW + DFe."
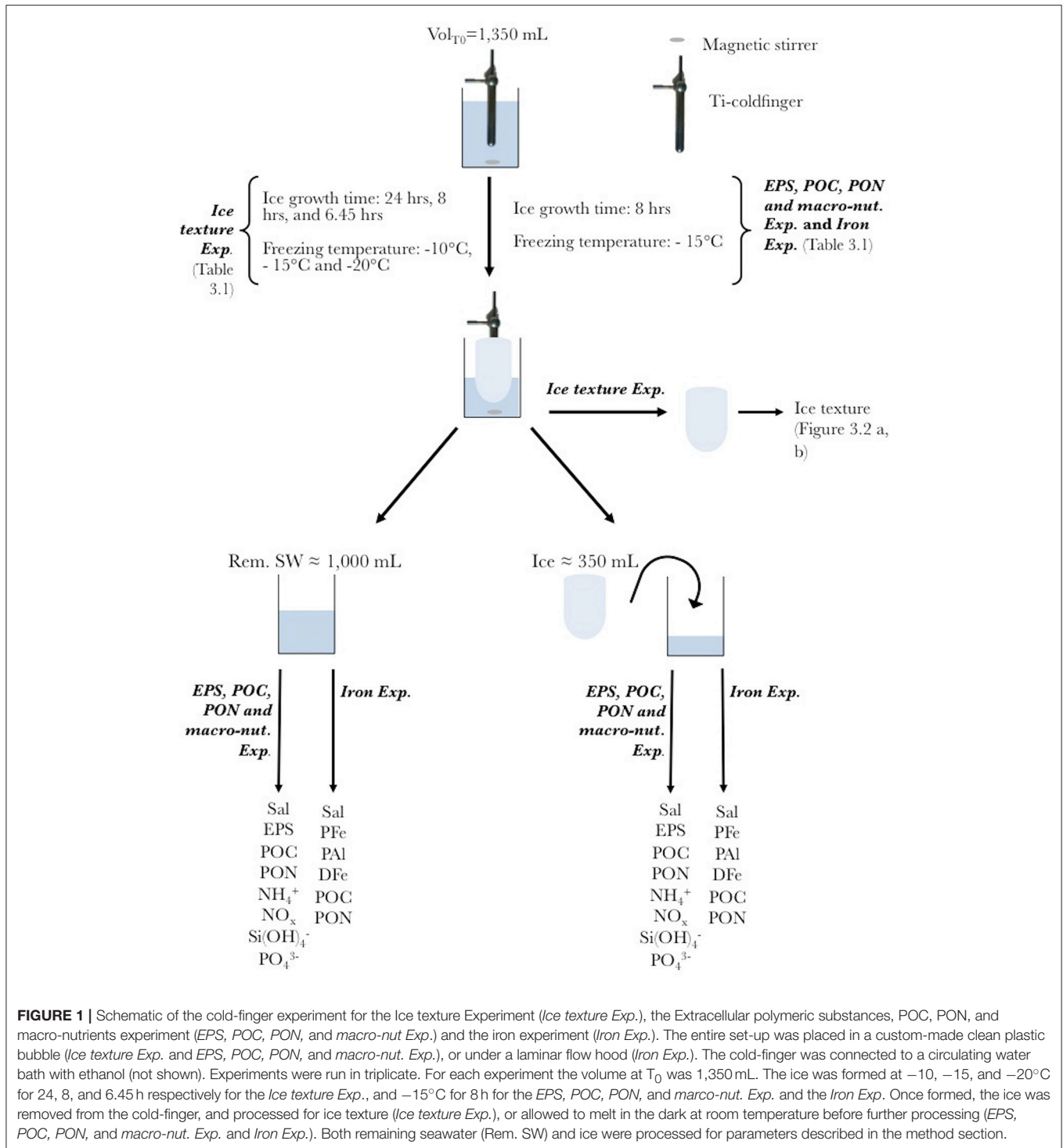
A final experiment was carried out using FSW to which 44 mL of melted bottom sea ice containing algae was added. The ice sample was collected at Davis station, Antarctica in November 2015 and maintained under optimum growth conditions in the IMAS culture room until the start of the experiment. This treatment, named "FSW + Algae," aimed at studying the incorporation of biogenic PFe in sea ice. A list of the treatments is given in **Table 1**.

Sea-Ice Growth Set-Up

The experimental set-up and manipulations were conducted in a custom-made clean plastic bubble in a 4°C cold room onboard RV *Polarstern* (*Ice texture Exp.*, *EPS, POC, PON, and macro-nut. Exp.*); and under a class-100 laminar flow hood (AirClean 600 PCR workstation, Model 300 Controller, AirClean System) in a 4°C cold room in the home-laboratory for experiments on the incorporation of Fe and organic matter (*Iron Exp.*). Ice was grown using a cold-finger apparatus first described by Kuiper et al. (2003) and Ewert and Deming (2011), modified for use under carbon and trace metal non-contaminant conditions. The cold-finger was fully made of titanium (Ti) and cooled with a circulating bath (Wise Circu, WCR-P22) using ethanol as coolant (**Figure 1**).

The cold-finger was immersed straight in a custom-cut square acid-clean 2 L PC container (Nalgene) filled with different source solutions of seawater (**Table 1**). The PC container was placed into an insulated box made of foam insulation sheet (TechLite®) and placed on a magnetic stirrer to insure the homogeneity of the source solutions during the experiments.

At the end of each 8-h experiment, the ice was carefully removed from the remaining seawater and extracted from the

FIGURE 1 | Schematic of the cold-finger experiment for the Ice texture Experiment (*Ice texture Exp.*), the Extracellular polymeric substances, POC, PON, and macro-nutrients experiment (*EPS, POC, PON,* and *macro-nut Exp.*) and the iron experiment (*Iron Exp.*). The entire set-up was placed in a custom-made clean plastic bubble (*Ice texture Exp.* and *EPS, POC, PON,* and *macro-nut. Exp.*), or under a laminar flow hood (*Iron Exp.*). The cold-finger was connected to a circulating water bath with ethanol (not shown). Experiments were run in triplicate. For each experiment the volume at T_0 was 1,350 mL. The ice was formed at −10, −15, and −20°C for 24, 8, and 6.45 h respectively for the *Ice texture Exp.*, and −15°C for 8 h for the *EPS, POC, PON,* and *marco-nut. Exp.* and the *Iron Exp.* Once formed, the ice was removed from the cold-finger, and processed for ice texture (*Ice texture Exp.*), or allowed to melt in the dark at room temperature before further processing (*EPS, POC, PON,* and *macro-nut. Exp.* and *Iron Exp.*). Both remaining seawater (Rem. SW) and ice were processed for parameters described in the method section.

cold-finger. Ice was allowed to melt at room temperature in an acid-clean PC container, following methods from Rintala et al. (2014). A diagram of the experimental set-up and workflow is shown in **Figure 1**. Both remaining seawater and melted ice were analyzed for the list of parameters described below. Prior to each treatment a T_0 sample was collected for measurements of the same parameters in the source solution.

Physical Variables: Salinity and Ice Texture

Salinities (practical salinity, S_P) of seawater, bulk ice (melted bulk-ice sample) and remaining seawater were measured using a portable salinity probe (YSI Incorporated model 30, precision ± 0.1). Vertical and horizontal thin sections of the ice were prepared following the method of Langway (1958). Thin sections were observed through 2 cross-polarized filters and

photographed following methods described in detail in Janssens et al. (2016).

Biogeochemical Variables
Extracellular Polymeric Substances
Melted ice and seawater samples were homogenized and filtered onto 25 mm diameter PC membranes (0.4 μm, Millipore) under low vacuum (<0.13 bar) to avoid cell lysis. Filters were stained with 500 μL of a solution of Alcian Blue (AB, GX8 Sigma, 0.02% AB in 0.06% acetic acid). Excess dye was removed by rinsing the membrane with 2 mL of UHP water (Millipore, Gradient A10). Membranes were then stored individually at −20°C in the dark until analysis. Concentrations were determined colorimetrically using the method of Passow and Alldredge (1995) and modified by van der Merwe et al. (2009). Concentrations were computed using the filter capture efficiency of 4% from van der Merwe et al. (2009).

Dissolved and Particulate Organic Material and Macro-Nutrients
All glassware used for POC and PON analysis were soaked in a 2% (v:v) HCl solution (analytical grade Merck EMSURE Germany), rinsed with UHP water, wrapped in aluminum foil and combusted at 450°C for 4 h. In between triplicates and treatments, glassware was rinsed with UHP water, soaked in a 2% (v:v) HCl solution (analytical grade, Merck EMSURE Germany) for 8 h and rinsed thoroughly with UHP water. Samples for POC and PON were filtered onto pre-combusted 25 mm quartz filters (Sartorius). A 20 mL subsample of the filtrate was collected and stored at −20°C in the dark until analysis for macro-nutrient concentrations (NO_x, $Si(OH)_4^-$, PO_4^{3-}, and NH_4^+). POC and PON samples were stored at −20°C in the dark until analysis. After acidification of the filters [30 μL of 10 % (v:v) HCl, Ajax Finichem] to remove inorganic carbon, POC and PON concentrations were determined using a Thermo Finnigan EA 1112 Series Flash Elemental Analyzer (precision 1%) at Central Science Laboratory (CSL, University of Tasmania). Silicic acid was analyzed using a photometric analyzer (Aquakem 250) and PO_4^{3-}, NO_x, and NH_4^+ were analyzed with a Lachat Flow injection analyzer following the methods of Grasshoff et al. (2009). Detection limits were 0.1 and 0.002 mg L^{-1} for each method, respectively.

Iron and Aluminum
All sampling LDPE bottles, PC containers, PC filtration sets, petri-dishes and other equipment in contact with the samples were cleaned following GEOTRACES recommendations (Cutter et al., 2017). Polycarbonate membranes for PFe and PAl were soaked in 10% (v:v) ultrapure HCl for a week, thoroughly rinsed with UHP water (Barnstead International, NANOpure Diamond polisher) and stored in UHP water until use. Before and between treatments and triplicates, the cold-finger was thoroughly rinsed with UHP water. Between triplicates, equipment used for Fe filtrations was thoroughly rinsed with UHP water, soaked in a 10% (v:v) HCl solution for 16 h and rinsed 5 times with UHP water.

Immediately after removing the ice from the PC bottle, the remaining seawater was filtered onto 0.4 μm pore size 47 mm diameter PC membrane filters (Sterlitech) using an acid-clean PC filtration set (Sartorius) under gentle vacuum (<0.13 bar). The filter was collected for measurements of PFe and PAl (particles > 0.4 μm) concentrations, and placed in acid-clean polystyrene petri-dishes. 60 mL of the filtrate was collected in LDPE bottles (Nalgene) and acidified to pH 1.8 with ultrapure HCl (Seastar from Choice Analytics) for DFe analysis. Once fully melted, the same process was applied to the melted sea ice. Filters were stored individually in acid-clean petri-dishes, triple bagged and kept at −20°C in the dark until analysis. The LDPE bottles containing the dissolved fraction were triple bagged and kept at ambient temperature until analysis.

Filters for PFe and PAl determination were digested using a mixture of strong acids following the method described in Bowie et al. (2010). Dissolved Fe samples were diluted 10 times to reduce sea salt matrix interferences effects during analysis. Particulate metals and DFe concentrations were then measured at the Central Science Laboratory (University of Tasmania) using a Sector Field Inductively Coupled Plasma Mass Spectrometer (ICP-MS, Element 2), following methods described in Bowie et al. (2010).

Segregation Coefficient and Enrichment Index
The partition coefficient, K_{eff} is used to describe the proportion of solute that is retained in sea ice.

$$K_{effX} = [X]_{ice}/[X]_{source}$$

where $[X]_{ice}$ and $[X]_{source}$ is the concentration of the component X in the ice and in the source solution, respectively.

To assess the enrichment of each component in the ice compared to sea salt, the enrichment index was calculated (EI_x, Gradinger and Ikävalko, 1998).

$$EI_x = [Sal]_{source}/[Sal]_{ice} \cdot [X]_{ice}/[X]_{source}$$

where $[Sal]_{source}$ is the salinity of the source solution, and $[Sal]_{ice}$ is the salinity of the ice. Enrichment index of 1, <1 or >1 will correspond to conservative, depletion or enrichment, respectively, of the component X as compared to bulk salinity.

Statistical Analysis
All statistical analyses were conducted using the statistical software R (version 3.3.3, R development Core Team, 2017). Differences in treatments were tested with standard analysis of variance (ANOVA) after log-transforming the response parameters to stabilize the variance (graphical diagnosis: Residuals vs. Fitted values, Normal quantiles vs. Standardized residuals, Scale location and Constant leverage). ANOVA was followed by a single-step multiple comparison Tukey-Honest Significant Differences (Tukey-HSD) procedure to determine which treatments differ. When the ANOVA showed no evidence of treatments differences for EIs, a t-test was performed to assess if the overall mean (of all treatments) of the EI was different from 1.

RESULTS

Ice Texture and Salinity

The ice texture was dominated by columnar ice (**Figures 2A,B**). The texture reflected the geometry of the cold-finger. Except for small differences in the size of the ice crystals, temperature had no effect on the geometry of the ice crystals.

Salinities of bulk-ice samples, as well as in the remaining seawater, were consistent throughout the experiments, with a mean bulk-ice salinity of 14.5 ± 1.3 S_P (mean $\pm$ standard deviation (SD), $n = 24$), and a mean salinity of 39.6 ± 1.3 ($n = 24$) for remaining seawater. The different growth temperatures applied to the samples resulted in similar partition coefficients (mean $K_{eff} = 0.32 \pm 0.07$, $n = 3$).

Extracellular Polymeric Substances, POC, PON, and Macro-Nutrients Experiments

Enrichment Indices of Macro-Nutrients and EPS

Figure 3 shows the enrichment indices for EPS and macro-nutrients in sea ice grown from Surface SW, Deep SW and Surface SW + XG. The horizontal line marks the EI = 1 (i.e., conservative incorporation). Results show that $Si(OH)_4^-$, NO_x, and PO_4^{3-} behave conservatively during sea-ice formation, whatever the source solution may be. Enrichment indices were close or equal to one for the macro-nutrients in Surface SW, Deep SW and Surface SW + XG (mean $\pm$ $SD = 1.0 \pm 0.09$, $n = 9$), except NH_4^+ that was enriched in the ice in each treatment. The largest signal was observed for NH_4^+, which is clearly enriched in sea ice compared to seawater, especially in the deep samples (**Figure 3**). We observed moderate evidence of a difference in incorporation of NH_4^+ between treatments (ANOVA $F = 5.28$, $P = 0.082$). A Tukey-HSD multiple comparison procedure showed that only the Deep SW and Surface SW + XG treatments could be distinguished ($P = 0.07$). EPS enrichment was variable and showed no significant differences (ANOVA $F = 2.03$, $P = 0.212$) between treatments. The highest EI_{EPS} was observed in the Surface SW treatment and the lowest EI_{EPS} was observed in the Deep SW treatment (**Figure 3**). The Deep SW experiment had the highest $EI_{NH_4^+}$ and also the lowest EI_{EPS}.

Enrichment Indices of POC and PON

All EI_{POC} and EI_{PON} were well above 1 indicating an enrichment of POC and PON in newly-formed ice (**Figure 4**). Mean EI_{POC} and EI_{PON} were 50.5 ± 35.7 ($n = 9$) and 8.9 ± 6.4 ($n = 9$), respectively. There is no evidence of treatment difference for EI_{POC} (ANOVA $F = 1.99$, $P = 0.186$), and strong evidence of treatment difference for EI_{PON} (ANOVA $F = 11.23$, $P = 0.005$; Tukey-HSD Surface SW + XG and Deep SW, $P = 0.038$; Tukey-HSD Surface SW + XG and Surface SW, $P = 0.005$).

Iron Experiments

Enrichment Indices of PFe and DFe

Figure 5 shows the enrichment indices for DFe and PFe in sea ice grown from the five different source solutions. The horizontal line marks the EI = 1 (i.e., conservative incorporation). Results show that DFe and PFe do not behave conservatively during sea-ice formation in any of the source solutions. Dissolved Fe was slightly enriched in sea ice compared to the source seawater solution in each treatment ($EI_{DFe} > 1$, t-test confidence level 95%, $P = 0.002$) and relatively stable between treatments (mean $EI_{DFe} = 2.2 \pm 0.9$, **Figure 5**) with no evidence that EI_{DFe} differed across treatment groups (ANOVA $F = 1.85$, $P = 0.196$).

We observed a strong evidence of difference in incorporation of PFe between treatments (ANOVA $F = 5.17$, $P = 0.035$). The UV-FSW + DFe and FSW + Algae treatments groups could be distinguished at the 0.05 level (Tukey-HSD, $P = 0.02$). Ice was enriched in PFe in the treatments where lithogenic or biogenic PFe was added: FSW + PFe ($EI_{PFe} = 1.3 \pm 1.41$, $n = 3$) and FSW + Algae ($EI_{PFe} = 4.7 \pm 2.8$, $n = 3$; **Figure 5**). When lithogenic PFe was added and UV treatment applied, less PFe was incorporated in sea ice (UV-FSW + PFe, $EI_{PFe} = 0.5 \pm 0.3$, $n = 3$) than without UV-treatment. The treatment where biogenic PFe was added (FSW + Algae) showed the highest EI_{PFe} of all treatments ($EI_{PFe} = 4.7 \pm 2.8$, $n = 3$).

Enrichment Indices of POC and PON

Particulate organic matter (POC and PON) was more enriched in sea ice in treatments where PFe was added than in treatments where DFe was added (EI_{POC}: ANOVA, $F = 23.14$, $P = 0.003$; and EI_{PON}: ANOVA, $F = 24.57$, $P = 0.000$). Unlike other parameters, POC was the only compound showing a higher EI in UV-treated than in its non-UV treated equivalent. The enrichment index of PON was always lower than EI_{POC} (ANOVA, $F = 4.48$, $P = 0.040$; **Figure 6**).

Overall, the FSW + DFe and UV-FSW + DFe treatments had the lowest EIs and the lowest variability with EI_{PON} of 1.1 ± 0.7, $n = 3$ and 0.8 ± 0.5, $n = 3$, respectively.

The treatments with addition of lithogenic and biogenic PFe, and no UV treatment (FSW + PFe and FSW + Algae) were the only ones where enrichment in all compounds (DFe, PFe, POC, and PON) was observed relative to the source solution (**Figures 5, 6**). This was not the case for the treatments where DFe was added (FSW + DFe and UV-FSW + DFe), or when UV light was applied, where, depending on the compound, enrichment or depletion was observed.

Particulate Fe to Particulate Al Ratios

Aluminum can be used as a tracer of lithogenic Fe inputs (Lannuzel et al., 2014a). The PFe/PAl molar ratio in the ice was elevated in all treatments compared to the Earth crustal ratio of 0.33 (Taylor, 1964). Two different patterns were observed: In the treatments with addition of PFe (FSW + PFe, UV-FSW + PFe and FSW + Algae), PFe/PAl was higher in the ice than in the remaining seawater (**Figure 7A**), however, this was not statistically significant (ANOVA $F = 0.68$, $P = 0.423$). In these treatments, the PFe/PAl ratios in the ice were up to 2 times higher than the crustal ratio (**Figure 7A**). In the treatment with DFe addition (FSW + DFe and UV-FSW + DFe) the PFe/PAl ratio in the ice was lower than in the remaining seawater (ANOVA $F = 9.60$, $P = 0.011$). In these experiments with addition of DFe, the PFe/PAl ratios were two to three orders of magnitudes higher than the crustal ratio (**Figure 7B**).
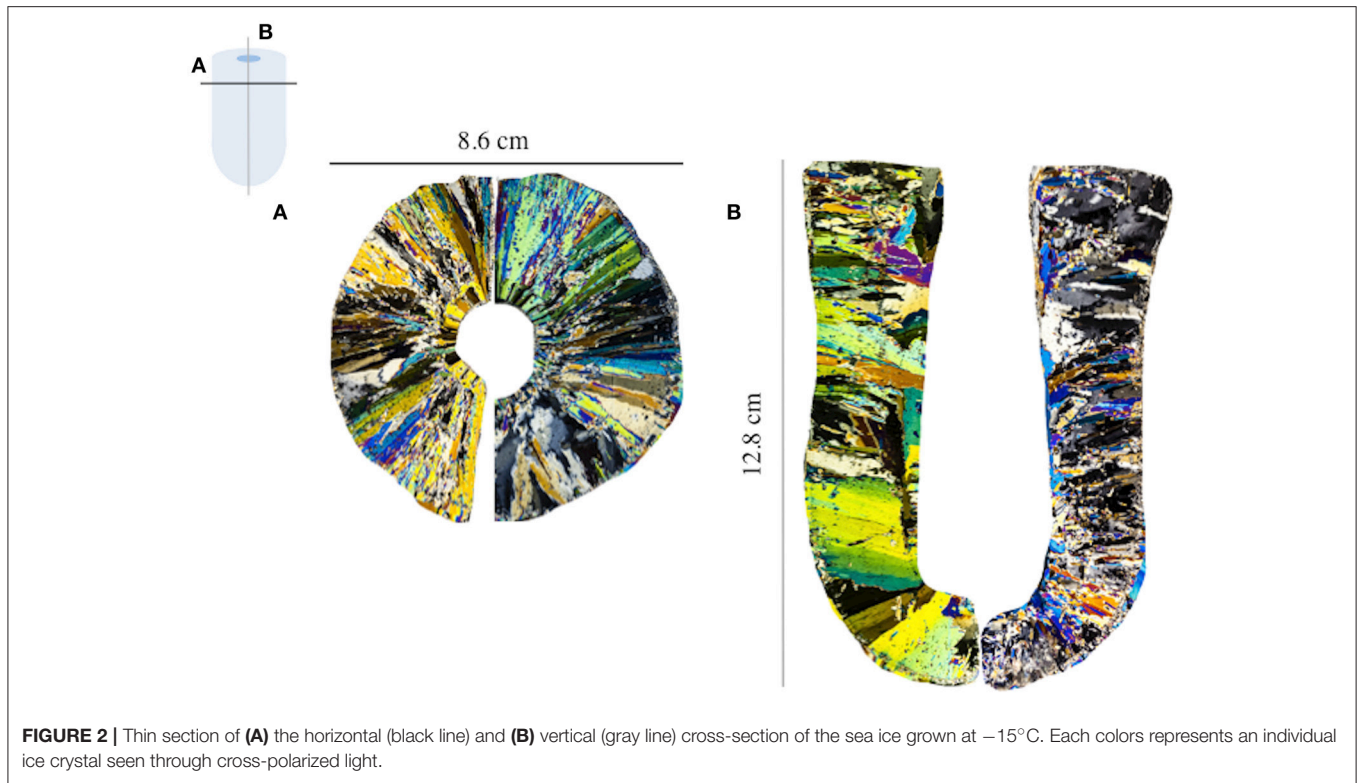
FIGURE 2 | Thin section of **(A)** the horizontal (black line) and **(B)** vertical (gray line) cross-section of the sea ice grown at -15°C. Each colors represents an individual ice crystal seen through cross-polarized light.
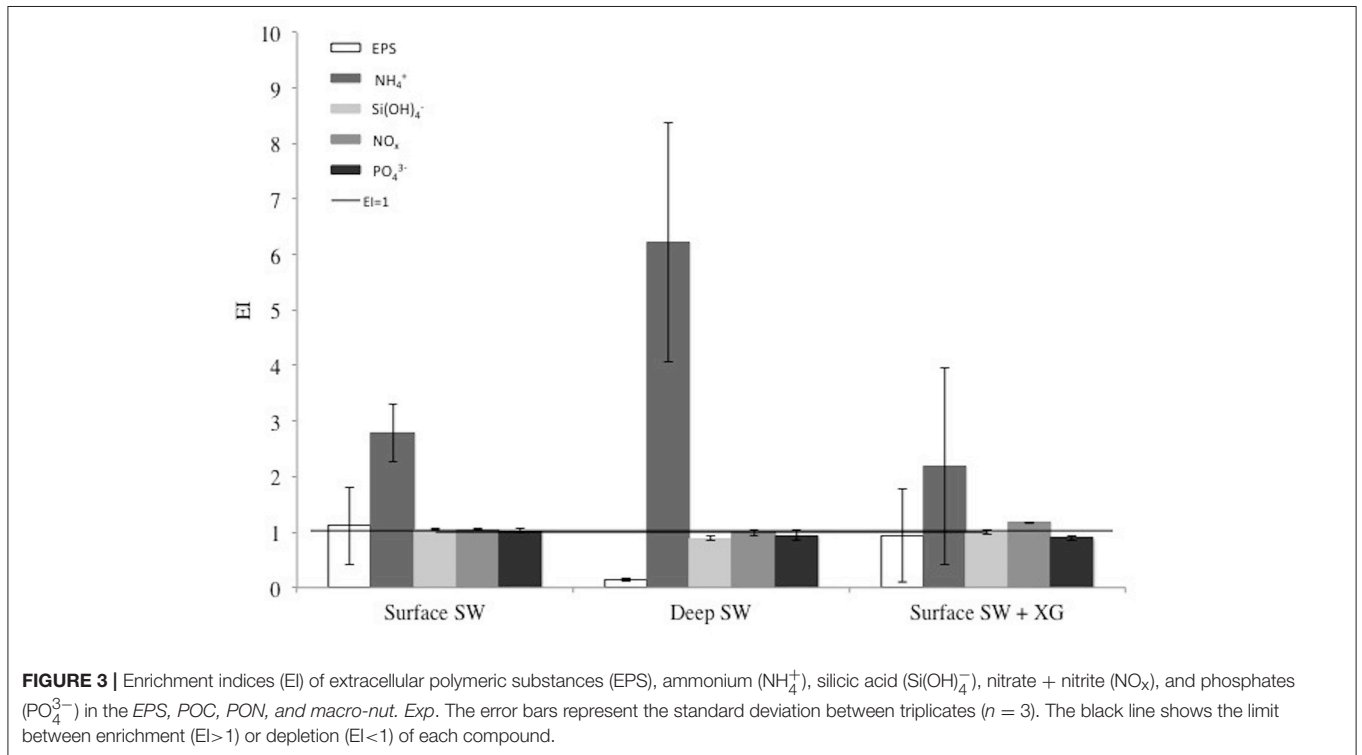

FIGURE 3 | Enrichment indices (EI) of extracellular polymeric substances (EPS), ammonium (NH_4^+), silicic acid ($Si(OH)_4^-$), nitrate + nitrite (NO_x), and phosphates (PO_4^{3-}) in the *EPS, POC, PON, and macro-nut. Exp*. The error bars represent the standard deviation between triplicates ($n = 3$). The black line shows the limit between enrichment (EI>1) or depletion (EI<1) of each compound.

DISCUSSION

The similarity in bulk ice and remaining seawater salinities between the different sets of experiments shows the reproducibility of our experimental set-up. Despite the unusual ice texture of the samples (horizontal ice crystals), representative processes of the natural environment are shown with the conservative behavior (i.e., relative to salt) of macro-nutrients,
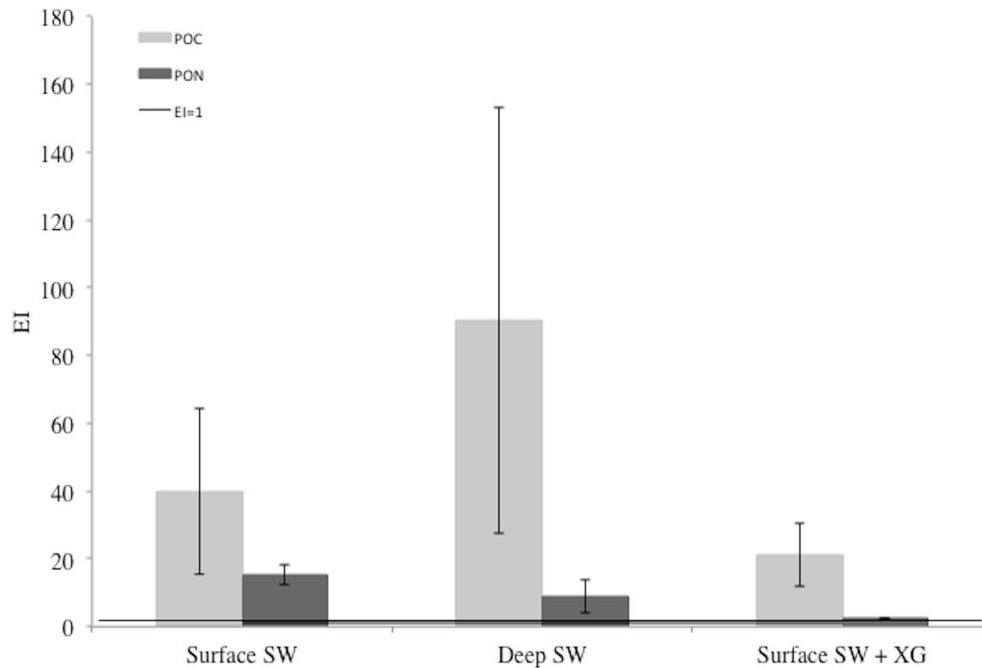
FIGURE 4 | Enrichment indices (EI) of particulate organic carbon (POC) and nitrogen (PON) in the *EPS, POC, PON,* and *macro-nut. Exp*. The error bars represent the standard deviation between triplicates (*n* = 3). The black line shows the limit between enrichment (EI>1) or depletion (EI<1) of POC or PON.
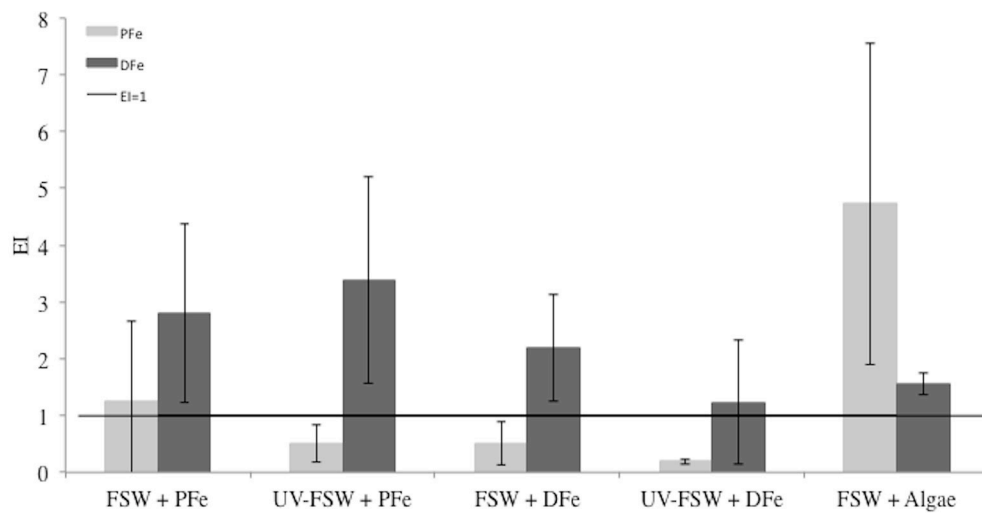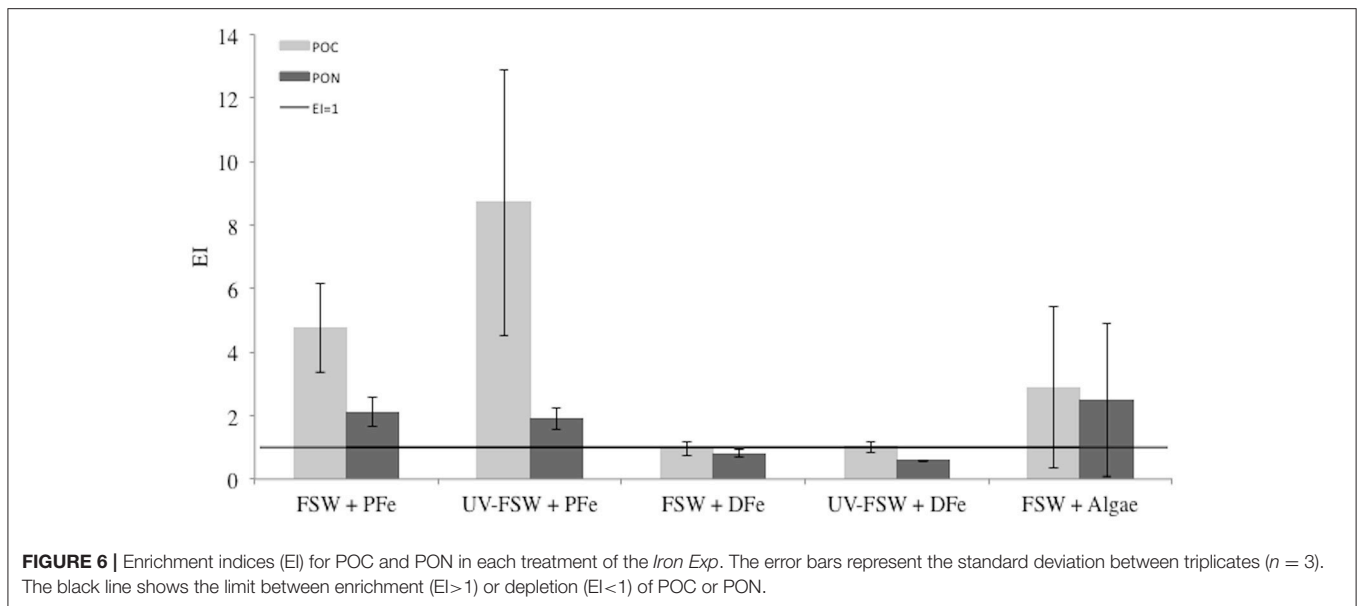

FIGURE 5 | Enrichment indices (EI) of particulate iron (PFe) and dissolved iron (DFe) in each treatment of the *Iron Exp*. The error bars represent the standard deviation between triplicates (*n* = 3). The black line shows the limit between enrichment (EI>1) or depletion (EI<1) of PFe or DFe.

except NH_4^+ as previously observed in natural young ice samples (Janssens et al., 2016) and sea-ice tank experiments (Zhou et al., 2014). In this study, the geometry of the ice crystal grown at 3 different temperatures in the *Ice texture Exp*. do not show any difference. This indicates that selection of the freezing temperature for the next set of experiments did not influence estimated EIs. The freezing temperature was chosen to resemble a realistic temperature encountered in the field in winter, but

was somewhat constrained by the minimum temperature of the circulating water bath.

Extracellular Polymeric Substances, POC, PON, and Macro-Nutrients Experiments
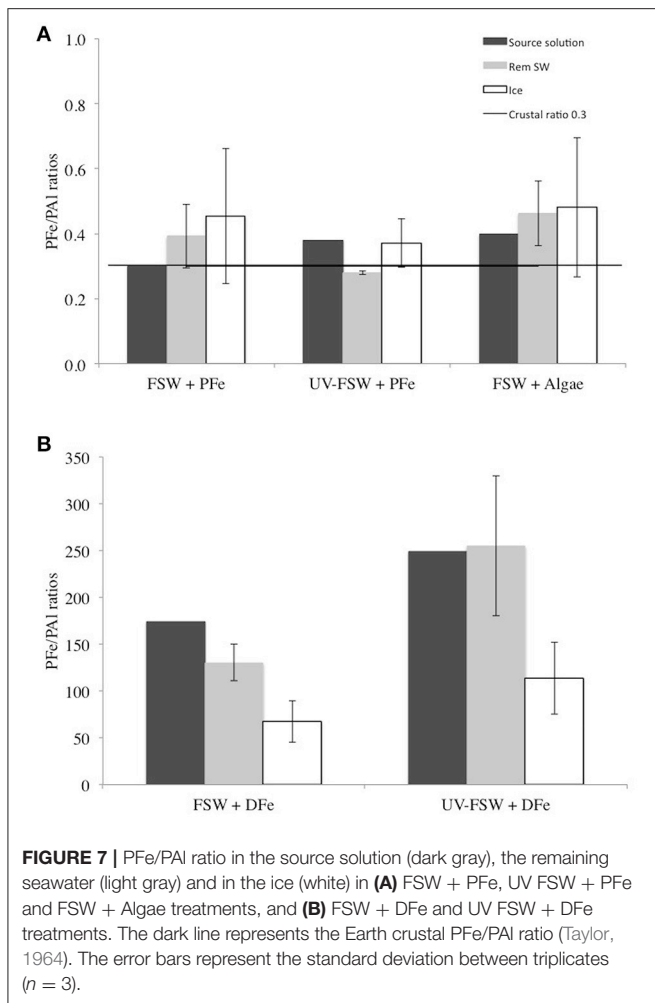### POC, PON, and EPS
EPS from deep seawater were the least enriched in the ice, although it had the highest initial concentration (0.10 μg xeq

FIGURE 6 | Enrichment indices (EI) for POC and PON in each treatment of the *Iron Exp*. The error bars represent the standard deviation between triplicates (*n* = 3). The black line shows the limit between enrichment (EI>1) or depletion (EI<1) of POC or PON.

L^{-1}). Also, the addition of XG, a reference standard for EPS in marine environments (Passow and Alldredge, 1995), did not show a preferential enrichment compared to the natural EPS in other treatments. Deep-sea bacteria have been found to produce EPS (Mancuso Nichols et al., 2005b), and it could be that deep-water EPS have different surface properties (e.g., number of anionic groups) or molecular weights than EPS produced in surface waters. Decho (1990) reported that physico-chemical characteristics of EPS are influenced by their tertiary structure, which is dependent on the frequency and type of functional groups presence on the EPS. This could also affect the incorporation efficiency, with stickier EPS being more enriched (Meiners and Michel, 2017). These divergences in surface properties of EPS could also play an important role in the incorporation of NH_4^+ in this experiment. The highest NH_4^+ enrichment was found when EI_{EPS} was the lowest (**Figure 3**). EPS have a negatively charged surface due to the high content of poly-anionic sugars. They are stabilized by the presence of cations (such as e.g., K^+ and Ca^{2+}) (Kloareg and Quatrano, 1988; Verdugo et al., 2004). Also, the sticky properties of EPS determine the interaction of EPS with other components of the marine environment (Passow, 2002). Some authors (e.g., Krembs et al., 2002a; Meiners and Michel, 2017) have suggested that the negatively charged EPS would complex with NH_4^+, and helped by their stickiness, lead to the enrichment of NH_4^+ and EPS in the ice (Fripiat et al., 2017). However, the lack of correlation between EPS and NH_4^+ in our study does not support this hypothesis, and further study is needed to decipher this process. Microbial regeneration of NH_4^+ has been previously observed in young sea ice (Riedel et al., 2007). However, due to the short duration of our experiment we believe microbial regeneration alone cannot fully explain the enrichment of NH_4^+ in the ice. In an ice tank study, Krembs et al. (2011) found that concentrations of EPS were higher in the ice when *Melosira arctica*, a diatom found in Arctic sea ice, was added to the source solution compared to ice

grown from saline solution containing different concentrations of XG, even if the concentration of XG was higher than the concentration of EPS produced by the diatom. Similarly, using a cold-finger apparatus similar to ours, Ewert and Deming (2011) showed that only native EPS produced by a cold-adapted marine bacterium (commonly found in sea ice) was preferentially incorporated in sea ice. Our results indicating that EPS from surface seawater are enriched in sea ice when compared to deep seawater are consistent with these previous findings, suggesting that the quality of EPS is a key parameter for its entrapment into sea ice.

Higher EI_{POC} than EI_{PON} are in line with previous reports of high POC and PON concentrations in young Antarctic sea ice (Janssens et al., 2016). In our laboratory study, POC and PON were more enriched in experiments using Antarctic unfiltered seawater compared with experiments conducted with filtered source solutions from Tasmania (*Iron* Exp.). The presence of biogenic material (phytoplankton, bacteria and EPS) in the unfiltered Antarctic sample could explain this higher enrichment compared to the filtered Tasmanian seawater sample. Also, similar to EPS, the quality of POC may control the degree of enrichment in sea ice. Due to its location, the coastal Tasmanian sampling site is under influence of terrestrial inputs bringing large amounts of allochtonous material to the pool of organic matter. This is in contrast to the Antarctic sampling sites, where the organic matter in the water column is mainly autochtonous. Zhou et al. (2014) showed that riverine DOM was less enriched in sea ice compared to autochtonous DOM, due to different molecular compositions, different affinity with other compounds, and with sea ice. Similarly, Müller et al. (2013) showed that the degree of dissolved organic carbon (DOC) enrichment depends on the chemical characteristics of the DOM. Our results suggest that the POC of potential terrestrial origin is less enriched in sea ice than the autochtonous Antarctic POC, by an order of magnitude. The reason why the POC is preferentially

FIGURE 7 | PFe/PAl ratio in the source solution (dark gray), the remaining seawater (light gray) and in the ice (white) in **(A)** FSW + PFe, UV FSW + PFe and FSW + Algae treatments, and **(B)** FSW + DFe and UV FSW + DFe treatments. The dark line represents the Earth crustal PFe/PAl ratio (Taylor, 1964). The error bars represent the standard deviation between triplicates ($n = 3$).

incorporated in the ice compared to PON remains unclear at this stage and this needs further investigations. One idea is EPS might have a higher POC/PON ratio or the organic matter in the ice comprises a mixed composition of live and dead material, with a higher carbon content relative to nitrogen.

Iron Experiments

Lithogenic vs. Biogenic Iron: Role of EPS Produced by Ice Algae and Bacteria

The EI_{PFe} in FSW + Algae was found to be up to 4 times higher than in any other treatment, suggesting a better incorporation of the biogenic PFe compared to the lithogenic PFe. The bottom ice sample added to the FSW + Algae treatment was dominated by pennate diatoms such a *Nitzschia stellata, N. lecointei, Fragillariopsis spec.,* and *Entomoneis kjellmanii* (Andreas Seger and Fraser Kennedy, personal communication). The large size of algal cells compared to the dust sample, may have lead to the preferential enrichment of biogenic PFe relative to lithogenic PFe. The added dusts were sieved through 20 μm nylon mesh, while mentioned diatom species can be as large as 150 μm in cell size (Scott and Marchant, 2005), and can also form colonies and

ribbon-chain like assemblages (Scott and Marchant, 2005; Aslam et al., 2012). Better incorporation of larger cells and impurities has been previously observed in natural young sea ice (Gradinger and Ikävalko, 1998; Riedel et al., 2007; Rózanska et al., 2008; Janssens et al., 2016).

Algal-bound EPS could also play a role in the incorporation of PFe into sea ice. Assemblages of diatoms are predominant in autotrophic-dominated sea-ice habitats and known to be associated to, and the main producers of, EPS (Krembs and Engel, 2001; Meiners et al., 2003, 2004; Mancuso Nichols et al., 2005a,b; Underwood et al., 2010, 2013). Particulate EPS have been shown to be likely of algal origin and quickly enriched into sea ice (Meiners et al., 2003; Riedel et al., 2007). EPS enrichment has been previously observed in cold-finger (Ewert and Deming, 2011) and ice tank experiments (Krembs et al., 2011). Negatively charged EPS (Decho, 1990; Mancuso Nichols et al., 2005a) are considered to be important in binding cationic metals like Fe^{3+} and Fe^{2+}. In return, Fe provides some stability to the EPS network by acting as bridging ions (e.g., Brown and Lester, 1982; Decho, 1990).

Finally, EPS are two to four orders of magnitude stickier than other particles (Passow, 2002), therefore potentially further helping the adhesion of PFe to ice surfaces. One can therefore assume that EPS were an important component of the added melted bottom ice sample to the source solution in the FSW + Algae treatment, contributing to the preferential enrichment in biogenic PFe compared to lithogenic PFe. Krembs et al. (2011) showed that the presence of EPS in the ice changes the microstructure of the ice and alters it physical properties. Thus, it is also possible that these modified properties are beneficial for PFe incorporation (more adapted shape of the pores and an increased internal sea ice surface area) but this requires further investigation.

The DFe fraction was less affected by the addition of algae than the PFe fraction. EPS range in size from sub-microns to hundreds of microns in the marine environment (Passow and Alldredge, 1995). EPS produced by sea-ice algae are known to be in the colloidal and soluble form (Aslam et al., 2012). In this study, a size distinction of 0.4 μm was used to define the dissolved and particulate fractions. This definition is however operationally defined and organic matter actually consists of a size continuum spanning across the soluble, colloidal and particulate size fractions. The colloidal material is operationally in the dissolved fraction as it is defined as the fraction that can pass through a filter with pore size of 0.1 to 0.46 μm (Chin et al., 1998). van der Merwe et al. (2009) suggested that organically-bound DFe in the ice shows reduced loss to the water column when brine drainage occurs by being associated with particles or cells (Sunda, 2001). The retention of DFe by EPS could explain the lower EI_{DFe} in the UV-treated FSW + DFe experiment.

Effect of UV Treatment on Fe Incorporation Efficiency: Importance of Organic Ligands

When subject to high UV exposure, DOM is degraded and ultimately transformed into carbon dioxide (CO_2) and water (H_2O). The UV- and non UV-treated experiments aimed at understanding the role of organic matter, including organic

ligands such as EPS, in the incorporation of Fe into sea ice. It has been shown that photochemical reactions alter the concentration and reactivity of the organic ligands involved in the complexation/solubilisation of trace metals (Moffett, 1995). More specifically, photochemical reduction of organically bound Fe decreases ligand-binding strength, rendering the complexed Fe more labile and increasing its bioavailability (Barbeau et al., 2001).

In this study, Fe was added to seawater solutions after UV treatment. While results between UV and non-UV treatments were not statistically significant, different enrichment behaviors for Fe and organic matter were observed between UV-treated and non-UV treated source solutions. The lack of statistical significance is a result of the large variance of the data set compared to the limited size of the data set. Further studies are needed to elucidate the full impact of UV treatment on the incorporation of organic matter into sea ice.

Nevertheless, as expected, DFe (and PFe) enrichment decreased when UV treatment was applied to FSW + DFe. This experiment suggests that the presence and quality of organic matter influences the incorporation of DFe into growing sea ice. However, DFe enrichment increased when UV treatment was applied to FSW + PFe. In the former treatments, the DFe was not present in excess; as such precipitation of DFe into PFe was not observed (see section Conversion of Dissolved Fe to Particulate Form). It is suggested that, in the latter case, the UV treatment resulted in the release of dissolved organic ligands from the degradation of particulate organic matter. These "newly-formed" ligands were then able to complex DFe and carry DFe into sea ice leading to higher EI_{DFe} in UV-FSW + PFe than in FSW + PFe, where dissolved organic ligands were more sparse. The difference in enrichment efficiency of DFe in (UV-)FSW+ PFe and (UV-)FSW + DFe by a combined effect of "ligand saturation" and precipitation of DFe into PFe can be explained in this way (see section Conversion of Dissolved Fe to Particulate Form). The UV-broken bound effect might have been compensated by the production of new dissolved organic ligands available for DFe. However, not enough dissolved organic ligands were present in solution to keep the added $30 \mu M$ of DFe in solution in the FSW + DFe treatment. Free DFe remaining in seawater therefore precipitated into PFe (see section Conversion of Dissolved Fe to Particulate Form), leading to the high PFe/PAl ratios observed.

As observed in the case of DFe incorporation in the (UV-)FSW + DFe treatments, PFe enrichment decreased when UV treatment was applied to FSW + PFe and FSW + DFe. This indicates the role of organic matter in the incorporation of PFe in growing sea ice. Unlike EI_{PFe} and EI_{DFe}, EI_{POC} increased when UV treatment was applied to FSW + PFe. It has been proposed that UV-B radiation breaks down not only DOC but also POC (UNEP, 1999), although the effect of UV on particulate organic matter is not clearly defined. Results here show that UV could impact on the quality of POC (including EPS) leading to different incorporation behaviors. It is likely that the POC becomes smaller when UV is applied and is then more easily incorporated into the ice. This argument however contradicts what has been previously observed in the field, where large particles are preferentially

incorporated in sea ice (Gradinger and Ikävalko, 1998; Riedel et al., 2007; Lannuzel et al., 2014b; Janssens et al., 2016).

One explanation is that UV-radiation changes the physico-chemical properties of organic matter in a way that the PFe-organic matter binding capacity would be reduced, but the enrichment of POC would be favored. Organic-free PFe would therefore be hardly incorporated, while the UV-induced modifications in the POC facilitate its incorporation. It has been shown that the binding potential of EPS is greatly influenced by their physico-chemical properties (Krembs and Deming, 2008; Verdugo, 2012), which are likely to be altered by UV irradiation. Therefore, more than the size, the important factor for enrichment of particles would be their physico-chemical properties and the tertiary structure/molecular composition/shape of the particles. Zhou et al. (2014) suggested that organic matter is initially incorporated as particulate organic matter and then converted into DOM once in the ice. This process may be observed in the FSW + Algae treatment, with the transformation of POC into DOC by heterotrophic organisms, leading to lower EI_{POC} than in (UV-)FSW + PFe. However, we note that 8 h of incubation time may not be sufficient for significant transformation. Zhou et al. (2014) also showed that different quality of DOC impacts the incorporation efficiency. It is suggested that this mechanism is also applicable to particulate constituents as discussed in section Lithogenic vs. Biogenic Iron: Role of EPS Produced by Ice Algae and Bacteria.

Conversion of Dissolved Fe to Particulate Form

The PFe/PAl ratios measured in the samples can give an indication on the level of conversion of DFe into PFe. The addition of DFe into seawater led to very high PFe/PAl ratios in the FSW + DFe and UV-FSW + DFe experiments (**Figure 7B**). A significant amount of DFe ($30 \mu M$) was added to these 2 solutions, without addition of organic ligands (e.g., EDTA) to balance the addition of DFe and keep it in solution. Organic ligands can be produced *in situ* by sea-ice algae and bacteria (Lannuzel et al., 2015) or supplied externally from e.g., sediment resuspension (Croot and Johansson, 2000; Buck et al., 2007). EDTA is synthetically produced and is therefore not an adequate model ligand of the natural environment.

The conversion observed here of the non-organically bound excess of DFe into the PFe pool (Lannuzel et al., 2014a, 2015), leads to the high PFe/PAl ratios observed. This process was even more expressed in the UV-FSW + DFe treatment, where the UV exposure likely broke the bounds of the Fe-ligand complexes already present in the source solution before addition of DFe. The newly formed PFe and remaining DFe could be then less prone to incorporation into sea ice, as observed by lower EI_{PFe} and EI_{DFe}. Two explanations are possible: (1) As previously mentioned in the preceding section, biogenic PFe (low in these experiments) is preferentially enriched in the newly-formed ice compared to lithogenic PFe. A decoupling between biogenic and lithogenic PFe incorporation could be observed. EPS have been proposed to be acting as a "plug," retaining salinity in the ice (Krembs et al., 2011). If the biogenic PFe is incorporated first, helped by the association to, and then retained in the ice by EPS, the incorporation of lithogenic PFe might not be as efficient and

could reach a concentration threshold in the ice. The association of Fe with EPS, as well as the space available in the brine channel system would therefore determine the incorporation, retention, and threshold of PFe in the ice.

(2) Organic ligands may play a key role in transferring DFe from seawater to sea ice. Organically-bound Fe would take advantage of the properties of the particles it is attached to, to get trapped in the ice as discussed previously (section Effect of UV Treatment on Fe Incorporation Efficiency: Importance of Organic Ligands).

It is difficult to distinguish the contribution of each process in these experiments and it is likely a combination of both. We note that Fe concentrations in these experiments were above the range of concentrations encountered in the Southern Ocean, although they are in the range of concentration found in Antarctic fast ice (Grotti et al., 2001; van der Merwe et al., 2011a,b; Noble et al., 2013). All conclusions in this study are derived from a high concentration scenario in regards to added DFe and PFe, but nonetheless, our results provide key information on the general chemistry of the involved processes.

Limitations of Laboratory Ice-Growth Experiments

Laboratory experiments offer a unique opportunity to study ice growth from its initial stage of ice formation while the history of a natural ice floe is difficult to assess. Laboratory experiments allow the isolation of processes occurring at the onset of ice formation, and the study of the influence of specific parameters, while controlling others. Most importantly, replicate measurements are possible in the laboratory while field sampling of a natural ice floe always carries the uncertainty of high spatial heterogeneity (e.g., Meiners et al., 2012, 2017; Williams et al., 2015).

However laboratory based ice-growth experiments also present some drawbacks. First, ice growth is limited in space (a few cm^3) and time (a few hours). In the cold-finger case, the geometry of the system is different from natural ice. Ice crystals are mainly growing horizontally (**Figure 2**), while natural columnar ice exhibits vertical ice crystals. Nonetheless, the good agreement between laboratory-based results and field studies shows that the initial incorporation of solutes and particles over a short period of time is not affected by the geometry of the ice. The cold-finger set-up is, therefore, a useful tool to complete field data and isolate processes to gain a mechanistic understanding of sea-ice biogeochemical processes.

CONCLUSION

This study represents the first study of processes of Fe enrichment in sea ice under laboratory conditions. The investigation suggests an important role of EPS and POC in the enrichment of PFe in sea ice. Results also indicated that large particles of biogenic PFe derived from sea ice algae are preferentially enriched compared to smaller particles of lithogenic PFe derived from continental dust. Combined these results indicate that rather than the quantity, it is the quality of EPS and POC that determines their rate of entrapment in the ice, with autochtonous POC being more enriched than allochtonous POC. The mechanisms remain unclear, but characterizations of these particles would be a step forward to understand the complex links between Fe and organic matter incorporation into sea ice. The quality of particulate organic matter determines its association with PFe, and ultimately the efficiency of PFe incorporation in sea ice. UV treatment likely alters organic matter and modifies its association with Fe (PFe and DFe). This ultimately affects their degree of enrichment. In the context of changing sea-ice environments, it is important to clearly identify the drivers and to quantify the processes that affect ice-associated Fe and carbon biogeochemical cycling in polar waters.

REFERENCES

Arzel, O., Fichefet, T., and Goosse, H. (2006). Sea ice evolution over the 20th and 21th centuries as simulated by current AOGCMs. *Ocean Model* 12, 401–415. doi: 10.1016/j.ocemod.2005.08.002

Aslam, S. N., Cresswell-Maynard, T., Thomas, D. N., and Underwood, G. J. C. (2012). Production and characterization of the intra- and extracellular carbohydrates and polymeric substances (EPS) of three sea-ice diatom species, and evidence for a cryoprotective role for EPS. *J. Phycol.* 48, 1494–1509. doi: 10.1111/jpy.12004

Barbeau, K., Rue, E. L., Bruland, K. W., and Butler, A. (2001). Photochemical cycling of iron in the surface ocean mediated by microbial iron(III)-binding ligands. *Nature* 413, 409–413. doi: 10.1038/35096545

Bowie, A. R., Townsend, A. T., Lannuzel, D., Remenyi, T. A., and van der Merwe, P. (2010). Modern sampling and analytical methods for the determination of trace elements in marine particulate material using magnetic sector inductively coupled plasma-mass spectrometry. *Anal. Chim. Acta* 676, 15–27. doi: 10.1016/j.aca.2010.07.037

Brown, M. J., and Lester, J. N. (1982). Role of bacterial extracellular polymers in metal uptake in pure culture and activated sludge-1. Effect of metal concentration. *Water Res.* 16, 1539–1548. doi: 10.1016/0043-1354(82)90206-8

Buck, K. N., Lohan, M. C., Berger, C. J. M., and Bruland, K. W. (2007). Dissolved iron speciation in two distinct river plumes and an estuary: implications for riverine iron supply. *Limnol. Oceanogr.* 52, 843–855. doi: 10.4319/lo.2007.52.2.0843

Chin, W.-C., Orellana, M. V., and Verdugo, P. (1998). Spontaneous assembly of marine dissolved organic matter into polymer gels. *Nature* 391, 568–572. doi: 10.1038/35345

Croot, P. L., and Johansson, M. (2000). Determination of iron speciation by cathodic stripping voltammetry in seawater using the competing ligand. *Electroanalysis* 12, 565–576. doi: 10.1002/(SICI)1521-4109(200005)12:8<565::AID-ELAN565>3.0.CO;2-L

Cutter, G., Andersson, P., Codispoti, L., Croot, P., Francois, R., Lohan, M., et al. (2017). Sampling and sample-handling protocols for GEOTRACES cruises. Available at: http://www.geotraces.org/libraries/documents/Intercalibration/Cookbook.pdf

Decho, A. W. (1990). Microbial exopolymer in ocean environments: their roles in food webs and marine processes. *Ocean Mar. Biol. Annu. Rev.* 28, 73–153.

de Jong, J., Schoemann, V., Maricq, N., Mattielli, N., Langhorne, P., Haskell, T., et al. (2013). Iron in land-fast sea ice of McMurdo Sound derived from sediment resuspension and wind-blown dust attributes to primary productivity in the Ross Sea, Antarctica. *Mar. Chem.* 157, 24–40. doi: 10.1016/j.marchem.2013.07.001

de Jong, J. T. M., Stammerjohn, S. E., Ackley, S. F., Tison, J.-L., Mattielli, N., and Schoemann, V. (2015). Sources and fluxes of dissolved iron in the Bellingshausen Sea (West Antarctica): the importance of sea ice, icebergs and the continental margin. *Mar. Chem.* 177, 518–535. doi: 10.1016/j.marchem.2015.08.004

Else, B., Rysgaard, S., Attard, K., Campbell, K., Crabeck, O., Galley, R., et al. (2015). Under-ice eddy covariance flux measurements of heat, salt, momentum, and dissolved oxygen in an artificial sea ice pool. *Cold Reg. Sci. Technol.* 119, 158–169. doi: 10.1016/j.coldregions.2015.06.018

Ewert, M., and Deming, J. W. (2011). Selective retention in saline ice of extracellular polysaccharides produced by the cold-adapted marine bacterium Colwellia psychrerythraea strain 34H. *Ann. Glaciol.* 52, 111–117. doi: 10.3189/172756411795931868

Fripiat, F., Meiners, K. M., Vancoppenolle, M., Papadimitriou, S., Thomas, D. N., Ackley, S. F., et al. (2017). Macro-nutrients concentrations in Antarctic paci ice: overall patterns and overlooked processes. *Elem. Sci. Anthr.* 5:13. doi: 10.1525/elementa.217

Galley, R., Else, B., Geilfus, N.-X., Hare, A., Isleifson, D., Ryner, L., et al. (2013). Morphology and distribution of liquid inclusions in young sea ice as imaged by magnetic resonance. *Cryosph. Discuss.* 7, 4977–5006. doi: 10.5194/tcd-7-4977-2013

Geilfus, N.-X., Delille, B., Verbeke, V., and Tison, J.-L. (2012). Towards a method for high vertical resolution measurements of the partial pressure of CO_2 within bulk sea ice. *J. Glaciol.* 58, 287–300. doi: 10.3189/2012JoG11J071

Gradinger, R., and Ikävalko, J. (1998). Organism incorporation into newly forming Arctic sea ice in the Greenland Sea. *J. Plankton Res.* 20, 871–886. doi: 10.1093/plankt/20.5.871

Grasshoff, K., Kremling, K., and Ehrhardt, M. (2009). *Methods of Seawater Analysis, 3rd Edn.* Weinheim; New York, NY; Chiester; Brisbane, QLD; Singapore; Toronto, ON: Wiley-VCH.

Grotti, M., Soggia, F., Abelmoschi, M. L., Rivaro, P., Magi, E., and Frache, R. (2001). Temporal distribution of trace metals in Antarctic coastal waters. *Mar. Chem.* 76, 189–209. doi: 10.1016/S0304-4203(01)00063-9

Grotti, M., Soggia, F., Ianni, C., and Frache, R. (2005). Trace metals distributions in coastal sea ice of Terra Nova Bay, Ross Sea, Antarctica. *Antarct. Sci.* 17, 289–300. doi: 10.1017/S0954102005002695

Janssens, J., Meiners, K. M., Tison, J.-L., Dieckmann, G., Delille, B., and Lannuzel, D. (2016). Incorporation of iron and organic matter into young Antarctic sea ice during its initial growth stages. *Elem. Sci. Anthr.* 4:123. doi: 10.12952/journal.elementa.000123

Kloareg, B., and Quatrano, R. S. (1988). Structure of the cell walls of marine algae and ecophysiological functions of the matrix polysaccharides. *Oceanogr. Mar. Biol. Annu. Rev.* 26, 259–315.

Kovacs, A. (1996). *Sea Ice. Part 1. Bulk Salinity Versus Ice Floe Thickness.* CRREL report; 96-7. Hanover, NH: US Army Cold Regions Research and Engineering Laboratory.

Krembs, C., and Deming, J. W. (2008). "The role of exopolymers in microbial adaptation to sea ice," in *Psychrophiles: From Biodiversity to Biotechnology*, eds R. Margesin, F. Schinner, J. C. Marx, and C. Gerday (New York, NY: Springer-Verlag), 247–264.

Krembs, C., Eicken, H., and Deming, J. W. (2011). Exopolymer alteration of physical properties of sea ice and implications for ice habitability and biogeochemistry in a warmer Arctic. *Proc. Natl. Acad. Sci. U.S.A.* 108, 3653–3658. doi: 10.1073/pnas.1100701108

Krembs, C., Eicken, H., Junge, K., and Deming, J. W. (2002a). High concentrations of exopolymeric substances in Arctic winter sea ice: implications for the polar ocean carbon cycle and cryoprotection of diatoms. *Deep Res. Part I Oceanogr. Res.* 49, 2163–2181. doi: 10.1016/S0967-0637(02)00122-X

Krembs, C., and Engel, A. (2001). Abundance and variability of microorganisms and transparent exopolymer particles across the ice-water interface of melting first-year sea ice in the Laptev Sea (Arctic). *Mar. Biol.* 138, 173–185. doi: 10.1007/s002270000396

Krembs, C., Tuschling, K., and Juterzenka, K. (2002b). The topography of the ice-water interface - its influence on the colonization of sea ice by algae. *Polar Biol.* 25, 106–117. doi: 10.1007/s003000100318

Kuiper, M. J., Lankin, C., Gauthier, S. Y., Walker, V. K., and Davies, P. L. (2003). Purification of antifreeze proteins by adsorption to ice. *Biochem. Biophys. Res. Commun.* 300, 645–648. doi: 10.1016/S0006-291X(02)02900-5

Lancelot, C., de Montety, A., Goosse, H., Becquevort, S., Schoemann, V., Pasquer, B., et al. (2009). Spatial distribution of the iron supply to phytoplankton in the Southern Ocean: a model study. *Biogeosciences* 6, 4919–4962. doi: 10.5194/bgd-6-4919-2009

Langway, C. (1958). *Ice Fabrics and the Universal Stage.* Wilmette, IL: U.S. Snow, Ice and Permafrost Research Establishment.

Lannuzel, D., Chever, F., van der Merwe, P. C., Janssens, J., Roukaerts, A., Cavagna, A.-J., et al. (2014a). Iron biogeochemistry in Antarctic pack ice during SIPEX-2. *Deep Sea Res. Part II Top. Stud. Oceanogr.* 131, 111–122. doi: 10.1016/j.dsr2.2014.12.003

Lannuzel, D., Grotti, M., Abelmoschi, M. L., and van der Merwe, P. (2015). Organic ligands control the concentrations of dissolved iron in Antarctic sea ice. *Mar. Chem.* 174, 120–130. doi: 10.1016/j.marchem.2015.05.005

Lannuzel, D., Schoemann, V., de Jong, J., Chou, L., Delille, B., Becquevort, S., et al. (2008). Iron study during a time series in the western Weddell pack ice. *Mar. Chem.* 108, 85–95. doi: 10.1016/j.marchem.2007.10.006

Lannuzel, D., Schoemann, V., de Jong, J., Pasquer, B., van der Merwe, P., Masson, F., et al. (2010). Distribution of dissolved iron in Antarctic sea ice: spatial, seasonal, and inter-annual variability. *J. Geophys. Res.* 115:G03022. doi: 10.1029/2009JG001031

Lannuzel, D., Schoemann, V., de Jong, J., Tison, J.-L., and Chou, L. (2007). Distribution and biogeochemical behaviour of iron in the East Antarctic sea ice. *Mar. Chem.* 106, 18–32. doi: 10.1016/j.marchem.2006.06.010

Lannuzel, D., van der Merwe, P. C., Townsend, A. T., and Bowie, A. R. (2014b). Size fractionation of iron, manganese and aluminium in Antarctic fast ice reveals a lithogenic origin and low iron solubility. *Mar. Chem.* 161, 47–56. doi: 10.1016/j.marchem.2014.02.006

Lemke, P. and Participants of the ANT-XXIX/6 cruise. (2014). *The Expedition of the Research Vessel "Polarstern" to the Antarctic in 2013 (ANT-XXIX/6).* Berichte zur Polar-und Meeresforschung, Helmoltz Gemeinschaft, Bremerhaven, 679.

Loose, B., McGillis, W. R., Schlosser, P., Perovich, D., and Takahashi, T. (2009). Effects of freezing, growth, and ice cover on gas transport processes in laboratory seawater experiments. *Geophys. Res. Lett.* 36, 1–5. doi: 10.1029/2008GL036318

Mancuso Nichols, C. A., Garon Lardière, S., Bowman, J. P., Nichols, P. D., Gibson, J. A. E., and Guézennec, J. (2005a). Chemical characterization of exopolysaccharides from Antarctic marine bacteria. *Microb. Ecol.* 49, 578–589. doi: 10.1007/s00248-004-0093-8

Mancuso Nichols, C. A., Guezennec, J., and Bowman, J. P. (2005b). Bacterial exopolysaccharides from extreme marine environments with special

consideration of the Southern Ocean, sea ice, and deep-sea hydrothermal vents: a review. *Mar. Biotechnol.* 7, 253–271. doi: 10.1007/s10126-004-5118-2

Meiners, K., Brinkmeyer, R., Granskog, M. A., and Lindfors, A. (2004). Abundance, size distribution and bacterial colonization of exopolymer particles in Antarctic sea ice (Bellingshausen Sea). *Aquat. Microb. Ecol.* 35, 283–296. doi: 10.3354/ame035283

Meiners, K., Gradinger, R., Fehling, J., Civitarese, G., and Spindler, M. (2003). Vertical distribution of exopolymer particles in sea ice of the Fram Strait (Arctic) during autumn. *Mar. Ecol. Prog. Ser.* 248, 1–13. doi: 10.3354/meps248001

Meiners, K. M., Arndt, S., Bestley, S., Krumpen, T., Ricker, R., Milnes, M. et al. (2017). Antarctic pack ice algae distribution: floe-scale spatial variability and predictability from physical parameters. *Geophys. Res. Lett.* 44, 7382–7390. doi: 10.1002/2017GL074346

Meiners, K. M., and Michel, C. (2017). "Dynamics of nutrients, dissolved organic matter and exopolymers in sea ice," in *Sea Ice 3rd Edn,* ed D. N. Thomas (Chichester: John Wiley & Sons), 415–432.

Meiners, K. M., Vancoppenolle, M., Thanassekos, S., Dieckmann, G. S., Thomas, D. N., Tison, J.-L., et al. (2012). Chlorophyll a in Antarctic sea ice from historical ice core data. *Geophys. Res. Lett.* 39:L21602. doi: 10.1029/2012GL053478

Moffett, J. W. (1995). Temporal and spatial variability of copper speciation in the Sargasso Sea. *Deep Res. Part. I Oceanogr. Res.* 42, 1273–1295. doi: 10.1016/0967-0637(95)00060-J

Müller, S., Vähätalo, A. V., Stedmon, C. A., Granskog, M. A., Norman, L., Aslam, S. N., et al. (2013). Selective incorporation of dissolved organic matter (DOM) during sea ice formation. *Mar. Chem.* 155, 148–157. doi: 10.1016/j.marchem.2013.06.008

Noble, A. E., Moran, D. M., Allen, A. E., and Saito, M. A. (2013). Dissolved and particulate trace metal micronutrients under the McMurdo Sound seasonal sea ice: Basal sea ice communities as a capacitor for iron. *Front. Chem.* 1:25. doi: 10.3389/fchem.2013.00025

Passow, U. (2002). Transparent exopolymer particles (TEP) in aquatic environments. *Prog. Oceanogr.* 55, 287–333. doi: 10.1016/S0079-6611(02)00138-6

Passow, U., and Alldredge, A. L. (1995). A dye-binding assay for the spectrophotometric measurement of transparent exopolymer particles (TEP). *Limnol. Oceanogr.* 40, 1326–1335. doi: 10.4319/lo.1995.40.7.1326

Queroue, F., Townsend, A., van der Merwe, P., Lannuzel, D., Sarthou, G., Bucciarelli, E., et al. (2014). Advances in the offline trace metal extraction of Mn, Co, Ni, Cu, Cd, and Pb from open ocean seawater samples with determination by sector field ICP-MS analysis. *Anal. Methods* 6, 2837–2847. doi: 10.1039/C3AY41312H

Riedel, A., Michel, C., and Gosselin, M. (2006). Seasonal study of sea-ice exopolymeric substances on the Mackenzie shelf: implications for transport of sea-ice bacteria and algae. *Aquat. Microb. Ecol.* 45, 195–206. doi: 10.3354/ame045195

Riedel, A., Michel, C., Gosselin, M., and LeBlanc, B. (2007). Enrichment of nutrients, exopolymeric substances and microorganisms in newly formed sea ice on the Mackenzie shelf. *Mar. Ecol. Prog. Ser.* 342, 55–67. doi: 10.3354/meps342055

Rintala, J. M., Piiparinen, J., Blomster, J., Majavena, M., Müller, S., Uusikivi, J., et al. (2014). Fast direct melting of brackish sea-ice samples results in biologically more accurate results than slow buffered melting. *Polar Biol.* 37, 1811–1822. doi: 10.1007/s00300-014-1563-1

Rózanska, M., Poulin, M., and Gosselin, M. (2008). Protist entrapment in newly formed sea ice in the coastal Arctic Ocean. *J. Mar. Syst.* 74, 887–901. doi: 10.1016/j.jmarsys.2007.11.009

Scott, J. F., and Marchant, J. H. (2005). *Antarctic Marine Protists.* Canberra; Hobart: Australian Biological Ressources Study; Australian Antarctic Division.

Sedwick, P. N., and DiTullio, R. (1997). Regulation of algal blooms in Antarctic shelf waters by the release of iron from melting sea ice. *Geophys. Res. Lett.* 24, 2515–2518. doi: 10.1029/97GL02596

Sullivan, C. W., Arrigo, K. R., McClain, C. R., Comiso, J. C., and Firestone, J. (1993). Distributions of phytoplankton blooms in the Southern Ocean. *Science* 262, 1832–1837. doi: 10.1126/science.262.5141.1832

Sunda, W. G. (2001). "Bioavailability and bioaccumulation of iron in the sea," in *The Biogeochemistry of Iron in Seawater,* IUPAC Series on Analytical and physical chemistry of environment systems, eds D. R. Turner and K. H. Hunter (Chichester, UK; West Sussex: Wiley), 41–84.

Taylor, S. R. (1964). Abundance of chemical elements in the continental crust: a new table. *Geochim. Cosmochim. Acta* 28, 1273–1285. doi: 10.1016/0016-7037(64)90129-2

Underwood, G. J. C., Aslam, S. N., Michel, C., Niemi, A., Norman, L., Meiners, K. M., et al. (2013). Broad-scale predictability of carbohydrates and exopolymers in Antarctic and Arctic sea ice. *Proc. Natl. Acad. Sci. U.S.A.* 110, 15734–15739. doi: 10.1073/pnas.1302870110

Underwood, G. J. C., Fietz, S., Papadimitriou, S., Thomas, D. N., and Dieckmann, G. (2010). Distribution and composition of dissolved extracellular polymeric substances (EPS) in Antarctic sea ice. *Mar. Ecol. Prog. Ser.* 404, 1–19. doi: 10.3354/meps08557

UNEP (1999). *Executive Summary of the 1998 Report of the Environmental Assessment Panel, in Synthesis of the Reports of the Scientific, Environmental Effects, and Technologies and Economic Assessment Panels of the Montreal protocol,* UNEP, United Nations Environment Programme Ozone secretariat.

van der Merwe, P., Lannuzel, D., Bowie, A. R., Mancuso Nichols, C. A. and Meiners, K. M. (2011a). Iron fractionation in pack and fast ice in East Antarctica: temporal decoupling between the release of dissolved and particulate iron during spring melt. *Deep Sea Res II.* 58, 1222–1236. doi: 10.1016/j.dsr2.2010.10.036

van der Merwe, P., Lannuzel, D., Bowie, A. R., and Meiners, K. M. (2011b). High temporal resolution observations of spring fast ice melt and seawater iron enrichment in East Antarctica. *J. Geophys. Res.* 116:G03017. doi: 10.1029/2010JG001628

van der Merwe, P., Lannuzel, D., Mancuso Nichols, C. A., Meiners, K., Heil, P., Norman, L., et al. (2009). Biogeochemical observations during the winter–spring transition in East Antarctic sea ice: evidence of iron and exopolysaccharide controls. *Mar. Chem.* 115, 163–175. doi: 10.1016/j.marchem.2009.08.001

Verdugo, P. (2012). Marine microgels. *Ann. Rev. Mar. Sci.* 4, 375–400. doi: 10.1146/annurev-marine-120709-142759

Verdugo, P., Alldredge, A., Azam, F., Kirchman, D., Passow, U., and Santschi, P. (2004). The oceanic gel phase: a bridge in the DOM-POM continuum. *Mar. Chem.* 92, 67–85. doi: 10.1016/j.marchem.2004.06.017

Wang, S., Bailey, D., Lindsay, K., Moore, K., and Holland, M. (2014). Impacts of sea ice on the marine iron cycle and phytoplankton productivity. *Biogeosciences* 11, 4713–4731. doi: 10.5194/bg-11-4713-2014

Weissenberger, J., and Grossmann, S. (1998). Experimental formation of sea ice: importance of water circulation and wave action for incorporation of phytoplankton and bacteria. *Polar Biol.* 20, 178–188. doi: 10.1007/s003000050294

Williams, G., Maksym, T., Wilkinson, J., Kunz, K., Murphy, C., Kimball, P., et al. (2015). Thick and deformed Antarctic sea ice mapped with autonomous underwater vehicles. *Nat. Geosci.* 8, 61–67. doi: 10.1038/ngeo2299

Zhou, J., Delille, B., Eicken, H., Vancoppenolle, M., Brabant, F., Carnat, G., et al. (2013). Physical and biogeochemical properties in landfast sea ice (Barrow, Alaska): insights on brine and gas dynamics across seasons. *J. Geophys. Res.* 118, 3172–3189. doi: 10.1002/jgrc.20232

Zhou, J., Delille, B., Kaartokallio, H., Kattner, G., Kuosa, H., Tison, J.-L., et al. (2014). Physical and bacterial controls on inorganic nutrients and dissolved organic carbon during a sea ice growth and decay experiment. *Mar. Chem.* 166, 59–69. doi: 10.1016/j.marchem.2014.09.013